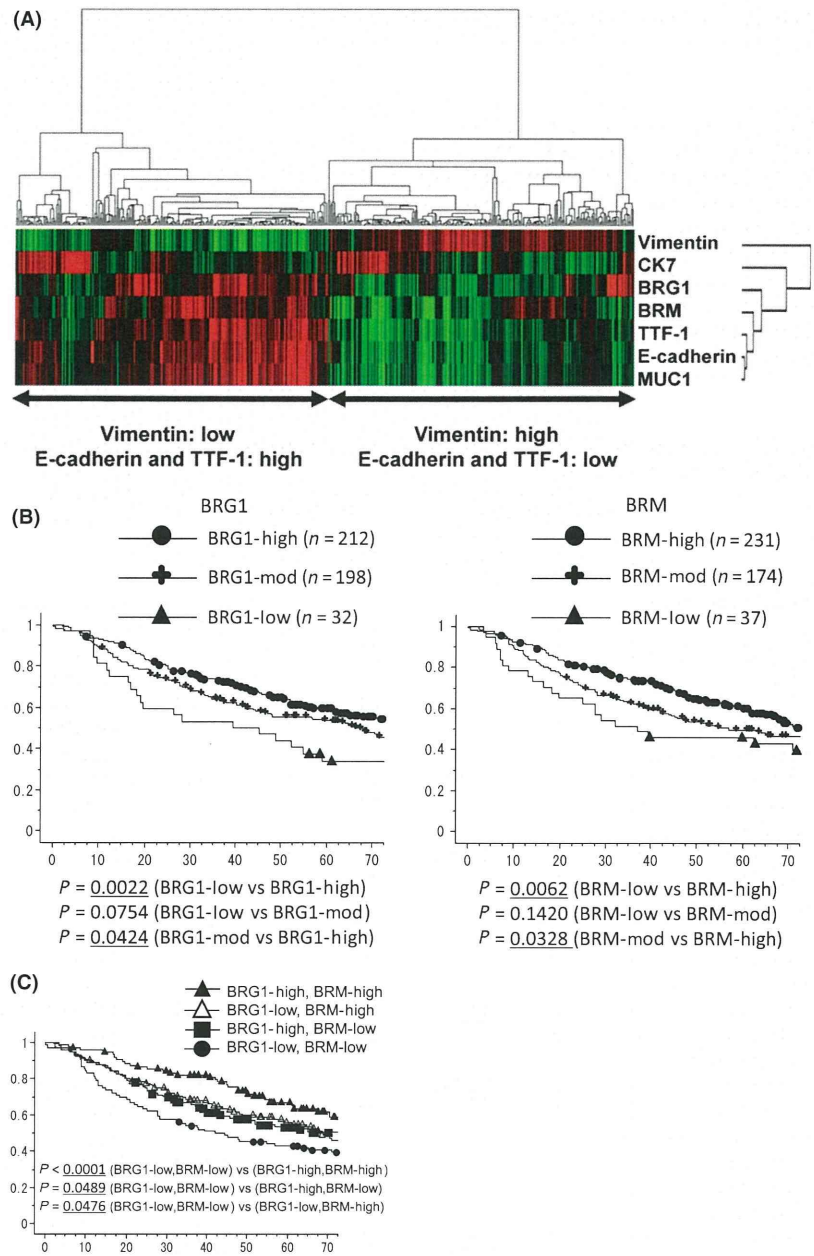

Fig. 5. Analysis of the publicly available data of 442 primary lung adenocarcinoma cases. (A) Hierarchical cluster analysis using the gene expressions of vimentin, CK7, BRG1, BRM, TTF-1, E-cadherin, and MUC1. (B) Patient survival according to the expression levels of BRG1 and BRM. Lung adenocarcinoma cases were separated into three groups based on gene expression levels of BRG1 and BRM: (i) cases with high expression (more than or equal to the average); (ii) cases with moderate expression (under the average, and more than or equal to half the average); and (iii) cases with low expression (under half the average). Left panel shows patient survival curves with high expression levels of BRG1 (BRG1-High), moderate expression levels of BRG1 (BRG1-Mod), and low expression levels of BRG1 (BRG1-Low). Right panel shows patient survival curves with high expression levels of BRM (BRM-High), moderate expression levels of BRM (BRM-Mod), and low expression levels of BRM (BRM-Low). (C) Patient survival according to the expression pattern of BRG1 and BRM. Patients were separated into four groups according to the expression pattern of BRG1 and BRM as follows: cases with high expression levels of both BRG1 and BRM (BRG1-High, BRM-High), cases with high expression levels of BRG1 and moderate or low expression levels of BRM (BRG1-High, BRM-Low), cases with moderate or low expression levels of BRG1 and high expression levels of BRM (BRG1-Low, BRM-High), the cases with moderate or low expression levels of both BRG1 and BRM (BRG1-Low, BRM-Low).

Discussion

This is, to our knowledge, the first report demonstrating the tight correlation between loss of BRG1 and BRM and EMT in cancer. Results of this study also confirm and reinforce our previous data that loss of the bronchial epithelial phenotype occurs in lung adenocarcinomas with EMT features.[13]

Recent studies show that loss of another component of the SWI/SNF chromatin remodeling complex, BAF250A (ARID1A), was frequent in high-grade endometrial carcinomas and clear cell carcinomas of the ovary[16] and that loss of the BAF250A protein correlates with the ARID1A mutation status.[17,18] Interestingly, there appears to be a similarity between loss of BRG1 and that of ARID1A; both tend to occur in high-grade tumors or in tumors with an altered epithelial phenotype.

Another interesting finding of this study was that features of TRU type lung adenocarcinomas,[14] that is, lepidic growth features, high expression levels of the TTF-1 protein, and EGFR mutations were absent in all cases with loss of the BRG1 protein. In tumors with BRG1 loss, BRG1 protein expression was typically absent in almost all cancer cells. These results suggest that loss of BRG1 occurs at an early step of carcinogenesis of lung adenocarcinoma with the mesenchymal-like phenotype, that is, a subset of non-TRU type lung adenocarcinomas with EMT features.

All cases with concomitant loss of BRG1 and BRM were devoid of lepidic growth components, harbored no EGFR mutations, and correlated more with solid adenocarcinoma morphology than a single loss of BRG1 or BRM, which suggested that loss of BRM may also occur in a subset of the mesenchymal-like phenotype, simultaneously with, or subsequently to, loss of BRG1, and may accelerate poorer

© 2012 Japanese Cancer Association

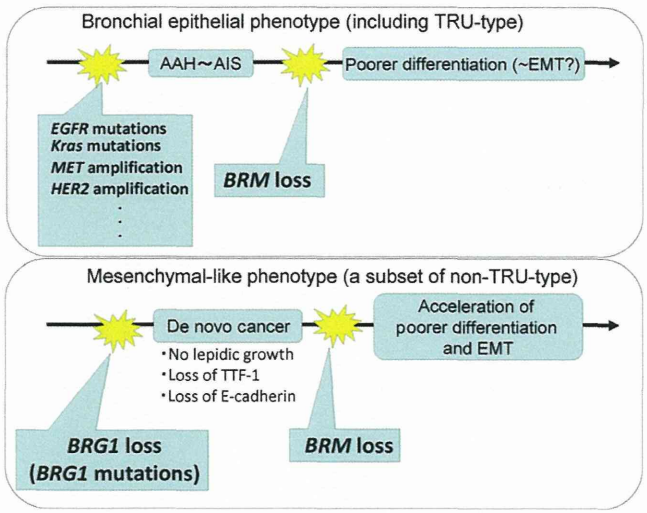

Fig. 6. Hypothetical schemes of BRG1 and BRM loss in the development of two types of lung adenocarcinomas: lung adenocarcinoma with the bronchial epithelial phenotype (upper panel) and lung adenocarcinoma with mesenchymal-like phenotype (lower panel).

differentiation and EMT and lead to the more malignant phenotype. The survival analysis of Shedden's data, which showed that cases with concomitant loss of BRG1 and BRM had poorer prognosis than cases with a single loss of BRG1, supports this hypothesis.

BRM expression was positive in lepidic growth components, but was weak or absent in invasive poorer differentiated lesions, such as solid components. In contrast to BRG1 loss, BRM loss may occur during the progressions of lung adenocarcinomas with the bronchial epithelial phenotype. Figure 6 shows our hypothetical schemes for BRG1 and BRM loss in the development of two types of lung adenocarcinomas: lung adenocarcinomas showing the bronchial epithelial phenotype and those showing the mesenchymal-like phenotype.

BRG1 and BRM regulate a broad range of genetic programs, including cell differentiation and proliferation, and it has been suggested that SWI/SNF complexes may dictate lineage-specific chromatin remodelling functions and act as master regulators of the master regulators.[4] Thus, although the exact mechanism by which loss of BRG1 and BRM leads to tumor development and EMT is unknown, loss of BRG1 and BRM may cause uncontrolled cellular proliferation and disrupt the differentiation program of bronchial epithelial cells,[19] resulting in formation of tumors with loss of expression of CK7, MUC1, and TTF-1. Why BRG1 loss occurs exclusively in the progression of EGFR wild-type tumor is currently unknown. One speculation could be that the simultaneous presence of EGFR mutation and BRG1 loss is for some reason incompatible with survival of cancer cells. Finally, we speculate that epigenetic therapy aiming to restore the functions of BRG1 and BRM would be a possible new therapy for treating tumors with EMT features.

Acknowledgments

This study was supported in part by the Smoking Research Foundation, the Foundation for Development of Community, the Vehicle Racing Commemorative Foundation, and the Ministry of Health, Labor and Welfare, and the Ministry of Education, Culture, Sports, Science and Technology of Japan. This publication was subsidized by JKA through its promotion funds from KEIRIN RACE. We thank Dr S. Matsukuma and Dr E. Tsuchiya, Molecular Pathology and Genetics Division, Kanagawa Cancer Center Research Institute, for technical advice on the loop-hybrid method.

Disclosure Statement

The authors have no conflict of interest.

References

1 Statistics and Information Department. *Vital Statistics, 2000*. Tokyo: Ministry of Health, Labor and Welfare, 2001.
2 Jemal A, Siegel R, Ward E *et al.* Cancer statistics, 2006. *CA Cancer J Clin* 2006; **56**: 106–30.
3 Janku F, Garrido-Laguna I, Petruzelka LB, Stewart DJ, Kurzrock R. Novel therapeutic targets in non-small cell lung cancer. *J Thorac Oncol* 2011; **6**: 1601–12.
4 Wilson BG, Roberts CW. SWI/SNF nucleosome remodellers and cancer. *Nat Rev Cancer* 2011; **11**: 481–92.
5 Jones S, Wang TL, Shih IM *et al.* Frequent mutations of chromatin remodeling gene ARID1A in ovarian clear cell carcinoma. *Science* 2010; **330**: 228–31.
6 Varela I, Tarpey P, Raine K *et al.* Exome sequencing identifies frequent mutation of the SWI/SNF complex gene PBRM1 in renal carcinoma. *Nature* 2011; **469**: 539–42.
7 Gui Y, Guo G, Huang Y *et al.* Frequent mutations of chromatin remodeling genes in transitional cell carcinoma of the bladder. *Nat Genet* 2011; **43**: 875–8.
8 Zang ZJ, Cutcutache I, Poon SL *et al.* Exome sequencing of gastric adenocarcinoma identifies recurrent somatic mutations in cell adhesion and chromatin remodeling genes. *Nat Genet* 2012; **44**: 570–4.
9 Medina PP, Romero OA, Kohno T *et al.* Frequent BRG1/SMARCA4-inactivating mutations in human lung cancer cell lines. *Hum Mutat* 2008; **29**: 617–22.
10 Glaros S, Cirrincione GM, Palanca A, Metzger D, Reisman D. Targeted knockout of BRG1 potentiates lung cancer development. *Cancer Res* 2008; **68**: 3689–96.
11 Reisman DN, Sciarrotta J, Wang W, Funkhouser WK, Weissman BE. Loss of BRG1/BRM in human lung cancer cell lines and primary lung cancers: correlation with poor prognosis. *Cancer Res* 2003; **63**: 560–6.
12 Fukuoka J, Fujii T, Shih JH *et al.* Chromatin remodeling factors and BRM /BRG1 expression as prognostic indicators in non-small cell lung cancer. *Clin Cancer Res* 2004; **10**: 4314–24.
13 Matsubara D, Ishikawa S, Sachiko O *et al.* Co-activation of epidermal growth factor receptor and c-MET defines a distinct subset of lung adenocarcinomas. *Am J Pathol* 2010; **177**: 2191–204.
14 Takeuchi T, Tomida S, Yatabe Y *et al.* Expression profile-defined classification of lung adenocarcinoma shows close relationship with underlying major genetic changes and clinicopathologic behaviors. *J Clin Oncol* 2006; **24**: 1679–88.
15 Shedden K, Taylor JM, Enkemann SA *et al.* Gene expression-based survival prediction in lung adenocarcinoma: a multi-site, blinded validation study. *Nat Med* 2008; **14**: 822–7.
16 Wiegand KC, Lee AF, Al-Agha OM *et al.* Loss of BAF250a (ARID1A) is frequent in high-grade endometrial carcinomas. *J Pathol* 2011; **224**: 328–33.
17 Wiegand KC, Shah SP, Al-Agha OM *et al.* ARID1A mutations in endometriosis-associated ovarian carcinomas. *N Engl J Med* 2010; **363**: 1532–43.
18 Maeda D, Mao TL, Fukayama M *et al.* Clinicopathological significance of loss of ARID1A immunoreactivity in ovarian clear cell carcinoma. *Int J Mol Sci* 2010; **11**: 5120–8.
19 Richly H, Lange M, Simboeck E, Di Croce L. Setting and resetting of epigenetic marks in malignant transformation and development. *BioEssays* 2010; **32**: 669–79.

doi: 10.1111/cas.12065
© 2012 Japanese Cancer Association

Supporting Information

Additional Supporting Information may be found in the online version of this article:

Data S1. Gene expression data of 19 cell lines.

Doc. S1. Supporting information about materials and methods.

Fig. S1. Gene and protein level expressions of BRG1, BRM, etc. of EGFR-mutated cell lines.

Fig. S2. Immunostaining for BRG1, BRM and E-cadherin in serial sections.

© 2012 Japanese Cancer Association

for patients who fail high dose chemoradiotherapy and autologous stem cell rescue for relapsed and primary refractory Hodgkin lymphoma. *British Journal of Haematology*, **146**, 158–163.

Moskowitz, A.J., Hamlin, P.A., Perales, M.A., Gerecitano, J., Horwitz, S.M., Matasar, M.J., Noy, A., Palomba, M.L., Portlock, C.S., Straus, D.J., Graustein, T., Zelenetz, A.D. & Moskowitz, C.H. (2013) Phase II study of bendamustine in relapsed and refractory Hodgkin lymphoma. *Journal of Clinical Oncology*, **31**, 456–460.

Younes, A., Oki, Y., Bociek, R.G., Kuruvilla, J., Fanale, M., Neelapu, S., Copeland, A., Buglio, D., Galal, A., Besterman, J., Li, Z., Drouin, M., Patterson, T., Ward, M.R., Paulus, J.K., Ji, Y., Medeiros, L.J. & Martell, R.E. (2011) Mocetinostat for relapsed classical Hodgkin's lymphoma: an open-label, single-arm, phase 2 trial. *The Lancet Oncology*, **12**, 1222–1228.

Zinzani, P.L., Viviani, S., Anastasia, A., Vitolo, U., Luminari, S., Zaja, F., Corradini, P., Spina, M., Brusamolino, E., Gianni, A.M., Santoro, A., Botto, B., Derenzini, E., Pellegrini, C. & Argnani, L. (2013) Brentuximab vedotin in relapsed/refractory Hodgkin's lymphoma: Italian experience and results of the use in the daily clinic outside clinical trials. *Haematologica*, **98**, 1232–1236.

Loss of CCR4 antigen expression after mogamulizumab therapy in a case of adult T-cell leukaemia-lymphoma

Adult T-cell leukaemia-lymphoma (ATL) is an aggressive peripheral T-cell neoplasm caused by human T-cell leukaemia virus type I infection. Most cases of aggressive ATL (acute, lymphoma, or unfavourable chronic type) are resistant to conventional chemotherapeutic agents, and, thus, it has a poor prognosis (Shimoyama, 1991; Tsukasaki *et al*, 2007). Therefore, development of alternative treatment strategies is an urgent issue. CC chemokine receptor 4 (CCR4) is expressed on most ATL cells and has been shown to be a new molecular target of immunotherapy *in vivo* (Ito *et al*, 2009). Mogamulizumab, a novel molecular targeting agent, is a humanized anti-CCR4 immunoglobulin G1 monoclonal antibody with a defucosylated Fc region, and 50% efficacy has been shown as a single agent in a phase II study for relapsed and refractory ATL (Ishida *et al*, 2012). We have little experience with this agent, as large-scale clinical studies have not been conducted. Here, we report an acute ATL case whose tumour cells lost CCR4 expression after administration of mogamulizumab.

A 63-year-old female was admitted to our hospital for fatigue, fever, skin eruption and hypercalcaemia, and was diagnosed with acute-type ATL. We started a dose-intensified chemotherapy of VCAP-AMP-VECP (vincristine, cyclophosphamide, doxorubicin, and prednisone; doxorubicin, ranimustine, and prednisone; and vindesine, etoposide, carboplatin, and prednisone) immediately. Six cycles were carried out, and partial remission was obtained, but the ATL cells remained in peripheral blood and skin lesions. ATL recurred with skin lesions immediately while myelosuppression was prolonged. Therefore, we started administration of mogamulizumab as a single agent, once per week for 8 weeks at a dose of 1·0 mg/kg. By the end of the treatment, complete remission was obtained with disappearance of ATL cells in peripheral blood, skin lesions, and normalization of lactate dehydrogenase levels. Unfortunately, a similar eruption developed approximately 3 months later, and the ATL relapsed. The patient again underwent mogamulizumab therapy, as she did not want further chemotherapy. However, the second administration had no effect, and the patient died due to disease progression.

We analysed CCR4 expression on patient ATL cells using multi-colour flow cytometry analysis, as described previously (Tian *et al*, 2011) to reveal the resistance mechanism. After dead cells (propidium iodide positive) and monocytes ($CD4^{dim}$ $CD14^{+}$) were gated out, a CD3 vs. CD7 plot of $CD4^{+}$ T cells was constructed, and CCR4 expression on the $CD3^{dim}$/$CD7^{low}$ subpopulation, in which ATL cells were highly enriched, was analysed. This analysis clearly revealed loss of CCR4 expression on ATL tumour cells after mogamulizumab therapy (Fig 1). Furthermore, we conducted clonal analysis by

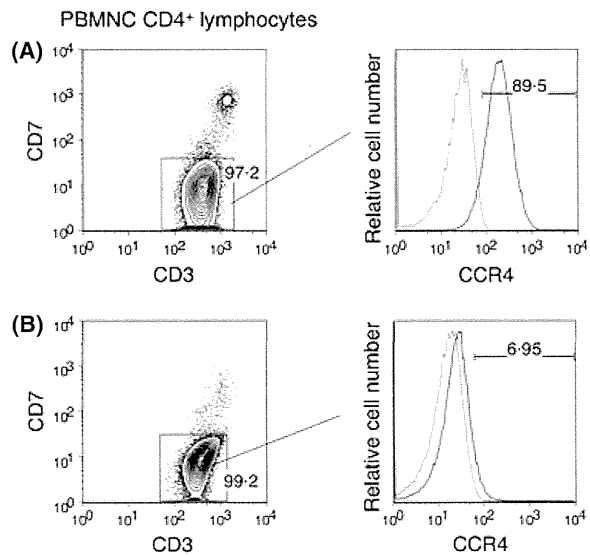

Fig 1. Multicolour flow cytometric analysis of CCR4 expression on adult T-cell leukaemia-lymphoma (ATL) cells. (A) Before mogamulizumab therapy. (B) After second mogamulizumab therapy. The ATL cells accumulated a $CD7^{low}$ subpopulation before and after treatment, without any change. Loss of the CC chemokine receptor 4 (CCR4) antigen was clearly observed after treatment.PBMNC, peripheral blood mononuclear cells.

© 2013 John Wiley & Sons Ltd

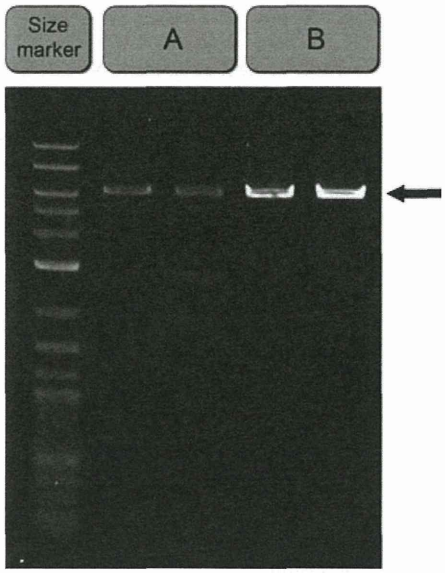

Fig 2. Clonal analysis by inverse long polymerase chain reaction (duplicated). (A) Before mogamulizumab therapy. (B) After second mogamulizumab therapy. The same monoclonal bands were observed before and after mogamulizumab therapy (arrow).

inverse long polymerase chain reaction (PCR) using the same sample. Genomic DNA extracted from peripheral blood mononuclear cells was digested with PstI. The purified DNA was self-ligated with T4 DNA ligase (Takara Bio, Otsu, Japan) and inverse long PCR was performed using Tks Gflex DNA Polymerase (Takara Bio) (Kobayashi *et al*, 2013). The PCRs were performed in duplicate. The band of the major clone was of identical size before and after mogamulizumab therapy (Fig 2), suggesting that the relapsed $CCR4^-$ ATL cells belonged to the same clone as the original $CCR4^+$ ATL cells.

To the best of our knowledge, this is the first report of loss of the CCR4 antigen by clonal analysis after mogamulizumab therapy. The resistance mechanism to mogamulizumab has not been elucidated to date. Mogamulizumab exerts its activity on CCR4-expressing T cells through an indirect effector mechanism, antibody-dependent cell-mediated cytotoxicity (ADCC) (Ishii *et al*, 2010). Thus, the CCR4 molecule itself could be involved in the resistance to mogamulizumab by loss of expression. It is believed that target molecular loss is not a rare phenomenon during monoclonal antibody therapy. For example, several reports are available regarding the loss of CD20 expression after the administration of rituximab, which is an anti-CD20 monoclonal antibody (Duman *et al*, 2012). Several mechanisms ranging from the gene to the protein level have been proposed to explain loss of CD20; a similar mechanism might cause loss of CCR4 expression. We demonstrated loss of CCR4 expression on the same ATL clone, which excluded the possibility of a clonal change by $CCR4^-$ ATL cells after mogamulizumab treatment. We have experienced another patient who became resistant to a second mogamulizumab administration but whose ATL cells maintained CCR4 expression. Loss of CCR4 expression is one of the resistance mechanisms to mogamulizumab; others include mutation or deletion within epitope-coding regions for mogamulizumab, increase in soluble CCR4, and reduced ADCC.

The anti-CCR4 antibody used in this study, clone 1G1, recognizes a distinct epitope from mogamulizumab (Ishii *et al*, 2010), which excluded the possibility of epitope masking by mogamulizumab. Our results indicate that CCR4 expression by ATL cells should be re-evaluated when relapsed patients with ATL are treated after mogamulizumab therapy even if their tumour cells express CCR4 at the initial evaluation.

Acknowledgements

We thank Ms. Eri Watanabe (Institute of Medical Science, The University of Tokyo) for technical assistance with flow cytometry. We are grateful to the hospital staff who are committed to providing high-quality care for all of our patients.

Author contributions

NO and KU wrote the manuscript. SK and TI performed the experiments using patient samples. KY, MK, and KS provided patient care and clinical information. NW supervized the flow cytometry. NO, AT, and KU supervized the research; and all authors approved the final manuscript.

Conflict of interest

The authors declare no financial conflict of interest.

Nobuhiro Ohno[1]
Seiichiro Kobayashi[2]
Tomohiro Ishigaki[2]
Koichiro Yuji[1]
Masayuki Kobayashi[2]
Koota Sato[2]
Nobukazu Watanabe[3]
Arinobu Tojo[1,2]
Kaoru Uchimaru[1]

[1]Department of Haematology/Oncology, Research Hospital, The Institute of Medical Science, The University of Tokyo, [2]Division of Molecular Therapy, The Institute of Medical Science, The University of Tokyo, and [3]Laboratory of Diagnostic Medicine, Division of Stem Cell Therapy, The Institute of Medical Science, The University of Tokyo, Tokyo, Japan
E-mail: nobuohno@ims.u-tokyo.ac.jp

Keywords: adult T-cell leukaemia-lymphoma, mogamulizumab, CC chemokine receptor 4, monoclonal antibody, flow cytometry

First published online 3 September 2013
doi: 10.1111/bjh.12555

© 2013 John Wiley & Sons Ltd

References

Duman, B.B., Sahin, B., Ergin, M. & Guvenc, B. (2012) Loss of CD20 antigen expression after rituximab therapy of CD20 positive B cell lymphoma (diffuse large B cell extranodal marginal zone lymphoma combination): a case report and review of the literature. *Medical Oncology*, **29**, 1223–1226.

Ishida, T., Joh, T., Uike, N., Yamamoto, K., Utsunomiya, A., Yoshida, S., Saburi, Y., Miyamoto, T., Takemoto, S., Suzushima, H., Tsukasaki, K., Nosaka, K., Fujiwara, H., Ishitsuka, K., Inagaki, H., Ogura, M., Akinaga, S., Tomonaga, M., Tobinai, K. & Ueda, R. (2012) Defucosylated anti-CCR4 monoclonal antibody (KW-0761) for relapsed adult T-cell leukemia-lymphoma: a multicenter phase II study. *Journal of Clinical Oncology*, **30**, 837–842.

Ishii, T., Ishida, T., Utsunomiya, A., Inagaki, A., Yano, H., Komatsu, H., Iida, S., Imada, K., Uchiyama, T., Akinaga, S., Shitara, K. & Ueda, R. (2010) Defucosylated humanized anti-CCR4 monoclonal antibody KW-0761 as a novel immunotherapeutic agent for adult T-cell leukemia/lymphoma. *Clinical Cancer Reserch*, **16**, 1520–1531.

Ito, A., Ishida, T., Utsunomiya, A., Sato, F., Mori, F., Yano, H., Inagaki, A., Suzuki, S., Takino, H., Ri, M., Kusumoto, S., Komatsu, H., Iida, S., Inagaki, H. & Ueda, R. (2009) Defucosylated anti-CCR4 monoclonal antibody exerts potent ADCC against primary ATLL cells mediated by autologous human immune cells in NOD/Shi-scid, IL-2R gamma(null) mice in vivo. *Journal of Immunology*, **183**, 4782–4791.

Kobayashi, S., Tian, Y., Ohno, N., Yuji, K., Ishigaki, T., Isobe, M., Tsuda, M., Oyaizu, N., Watanabe, E., Watanabe, N., Tani, K., Tojo, A. & Uchimaru, K. (2013) The CD3 versus CD7 plot in multicolor flow cytometry reflects progression of disease stage in patients infected with HTLV-I. *PLoS ONE*, **8**, 1–9.

Shimoyama, M. (1991) Diagnostic criteria and classification of clinical subtypes of adult T-cell leukaemia lymphoma. A report from the Lymphoma Study Group (1984-87). *British Journal of Haematology*, **79**, 428–437.

Tian, Y., Kobayashi, S., Ohno, N., Isobe, M., Tsuda, M., Zaike, Y., Watanabe, N., Tani, K., Tojo, A. & Uchimaru, K. (2011) Leukemic T cells are specifically enriched in a unique CD3(dim) CD7 (low) subpopulation of CD4(+) T cells in acute-type adult T-cell leukemia. *Cancer science*, **102**, 569–577.

Tsukasaki, K., Utsunomiya, A., Fukuda, H., Shibata, T., Fukushima, T., Takatsuka, Y., Ikeda, S., Masuda, M., Nagoshi, H., Ueda, R., Tamura, K., Sano, M., Momita, S., Yamaguchi, K., Kawano, F., Hanada, S., Tobinai, K., Shimoyama, M., Hotta, T., Tomonaga, M. & Japan Clinical Oncology Group Study JCOG9801. (2007) VCAP-AMP-VECP compared with biweekly CHOP for adult T-cell leukemia-lymphoma: Japan Clinical Oncology Group Study JCOG9801. *Journal of Clinical Oncology*, **25**, 5458–5464.

Correlating prothrombin time with plasma rivaroxaban level

Recently published guidelines from the British Committee for Standards in Haematology suggest that the prothrombin time (PT) can be used for urgent determination of anticoagulation intensity with rivaroxaban if a reagent with a known sensitivity is used (Baglin *et al*, 2012). However, it has been established in experiments using normal plasma spiked with varying concentrations of rivaroxaban that different PT reagents may have very different sensitivities to rivaroxaban (Samama *et al*, 2010; Douxfils *et al*, 2012). The clinical implications of this variation in PT sensitivity to rivaroxaban is evident from the recent report by Van Veen *et al* (2013), who described normal PTs in the presence of therapeutic rivaroxaban levels in a patient with renal impairment. Comparing the PT using Innovin® (Siemens, Marburg, Germany) and Thromborel S® (Siemens) in a patient commenced on rivaroxaban 15 mg twice daily for deep vein thrombosis against the rivaroxaban plasma concentration measured by the Biophen DiXal anti-Xa assay, they demonstrated normal PT results despite therapeutic plasma rivaroxaban levels. They concluded that PT results should be interpreted with caution when assessing coagulation intensity for patients on rivaroxaban (Van Veen *et al*, 2013). If available, a specific anti-Xa assay should be used for patients presenting with major bleeding or when requiring emergency surgery. Mueck *et al* (2011) have also demonstrated variation using Neoplastine® (Diagnostica Stago, Asnieres-sur-Seine, France) to measure the PT against rivaroxaban concentration.

However, many coagulation laboratories will not have 24-h access to a rivaroxaban-calibrated anti-Xa assay and will inevitably rely on their routine coagulation screen PT and activated partial thromboplastin time (APTT) results. Therefore it is essential that laboratories have knowledge of their reagents sensitivity to rivaroxaban. We studied the correlation between the rivaroxaban concentration (measured by Liquid Anti-Xa chromogenic assay, (Instrumentation Laboratory Company, Bedford, MA, USA) run on an IL TOP 700) and PT and APTT. The anti-Xa assay was calibrated using lyophilized standard rivaroxaban plasmas (Hyphen Biomed, Neuville-sur-Oise, France) to create a rivaroxaban assay linear between 0 and 400 ng/ml. Peak rivaroxaban plasma concentrations are considered to be in the range of 100–400 ng/ml, and trough concentrations in the range of 20–150 ng/ml (Baglin *et al*, 2012). PT (Recombiplastin 2G®, Instrumentation Laboratory Company, laboratory reference range 9–13 s) and APTT (Synthasil®, Instrumentation Laboratory Company, laboratory reference range 27–38 s) were determined on the IL TOP 700.

Blood samples (n = 33) were collected at random time points from 31 patients receiving rivaroxaban treatment for a minimum of 2 weeks. Fourteen results were obtained during 15 mg twice daily dosing and 19 during 20 mg once daily dosing. 19 blood samples were taken around the peak plasma concentration (1·0–5·5 h), 13 during trough periods (12–30 h) and for one patient, the sampling time was uncertain. The anti-Xa rivaroxaban concentrations during peak hours were marginally higher than was expected, with a median of 280 ng/ml (range 168–458). The trough levels were as expected, with a median of 57 ng/ml (range 11–215). There

© 2013 John Wiley & Sons Ltd

Cancer Science
The official journal of the Japanese Cancer Association

Adult T-cell leukemia cells are characterized by abnormalities of *Helios* expression that promote T cell growth

Satomi Asanuma,[1] Makoto Yamagishi,[1] Katsuaki Kawanami,[1] Kazumi Nakano,[1] Aiko Sato-Otsubo,[2] Satsuki Muto,[2] Masashi Sanada,[2] Tadanori Yamochi,[1] Seiichiro Kobayashi,[3] Atae Utsunomiya,[4] Masako Iwanaga,[5] Kazunari Yamaguchi,[6] Kaoru Uchimaru,[3] Seishi Ogawa[2] and Toshiki Watanabe[1,7]

[1]Graduate School of Frontier Sciences, The University of Tokyo; [2]Cancer Genomics Project, Graduate School of Medicine, The University of Tokyo; [3]Institute of Medical Science, The University of Tokyo, Tokyo; [4]Department of Hematology, Imamura Bun-in Hospital, Kagoshima; [5]Graduate School of Public Health, Teikyo University; [6]Department of Safety Research on Blood and Biological Products, National Institute of Infectious Diseases, Tokyo, Japan

(Received December 27, 2012/Revised April 11, 2013/Accepted April 15, 2013/Accepted manuscript online April 18, 2013/Article first published online May 19, 2013)

Molecular abnormalities involved in the multistep leukemogenesis of adult T-cell leukemia (ATL) remain to be clarified. Based on our integrated database, we focused on the expression patterns and levels of Ikaros family genes, *Ikaros*, *Helios*, and *Aiolos*, in ATL patients and HTLV-1 carriers. The results revealed profound deregulation of Helios expression, a pivotal regulator in the control of T-cell differentiation and activation. The majority of ATL samples (32/37 cases) showed abnormal splicing of Helios expression, and four cases did not express Helios. In addition, novel genomic loss in *Helios* locus was observed in 17/168 cases. We identified four ATL-specific short Helios isoforms and revealed their dominant-negative function. Ectopic expression of ATL-type Helios isoform as well as knockdown of normal Helios or Ikaros promoted T-cell growth. Global mRNA profiling and pathway analysis showed activation of several signaling pathways important for lymphocyte proliferation and survival. These data provide new insights into the molecular involvement of Helios function in the leukemogenesis and phenotype of ATL cells, indicating that Helios deregulation is one of the novel molecular hallmarks of ATL. (*Cancer Sci* 2013; 104: 1097–1106)

Adult T-cell leukemia (ATL) is a highly aggressive malignancy of mature CD4+ T cells and is caused by HTLV-1. After HTLV-1 infection, ATL is thought to develop following a multitude of events, including both genetic and epigenetic changes in the cells. Although many aspects of HTLV-1 biology have been elucidated, the detailed molecular mechanism of ATL leukemogenesis remains largely unknown.[1,2] Therefore, to precisely define the comprehensive abnormalities associated with ATL leukemogenesis, we previously carried out global mRNA and miRNA profiling of ATL cells derived from a large number of patients.[3,4] In this study, we focused on Ikaros family genes, especially Helios, on the basis of our integrated profiling of expression and gene copy number in ATL cells, which revealed the deregulated expression of this family of genes and genomic loss of *Helios* locus.

Ikaros family genes are specifically expressed in the hematopoietic system and play a vital role in regulation of lymphoid development and differentiation.[5–11] In addition, they are known to function as tumor suppressors during leukemogenesis according to several genetic studies carried out in mouse models.[12–15] Recently, many studies reported the deregulated splicing of Ikaros and the deletion of *Ikaros* locus in several human leukemias.[16–23] These abnormalities are associated with poor prognoses.[24–27] Helios is mainly expressed in the T-cell lineage.[10,11] Genomic changes and abnormal expression of Helios are also observed in some patients with T-cell malignancies.[18,28–31] However, in contrast to Ikaros, the substantial impact of aberrant Helios expression remains to be elucidated because of the absence of functional information, including the target genes of Helios.

In this study, we carried out a detailed expression analysis of Ikaros family genes in a large panel of clinical samples from ATL patients and HTLV-1 carriers and consequently identified a novel molecular characteristic, that is, abnormal splicing of Helios and loss of expression, which seems to be a significant key factor in leukemogenesis affecting the regulation of T-cell proliferation.

Materials and Methods

Cell lines and clinical samples. HeLa and 293T cells were cultivated in DMEM supplemented with 10% FCS. Human leukemic T cells, Jurkat, Molt-4, and CEM, ATL-derived, MT-1 and TL-Om1, and HTLV-1-infected MT-2 and Hut-102 cell lines were all maintained in RPMI-1640 with 10% FCS. The PBMCs from ATL patients of four clinical subtypes[32] and healthy volunteers were a part of those collected with informed consent as a collaborative project of the Joint Study on Prognostic Factors of ATL Development. The project was approved by the Institute of Medical Sciences, University of Tokyo Human Genome Research Ethics Committee (Tokyo, Japan). Clinical information of ATL individuals is provided in Table S1.

RNA isolation and RT-PCR analysis. The preparation of total RNA and synthesis of the first strand of cDNA were described previously.[3] The mRNAs of Ikaros family genes were examined by PCR with Platinum Taq DNA Polymerase High Fidelity (Invitrogen, Carlsbad, CA, USA). The PCR products were sequenced by automated DNA sequencer. Nested PCR amplification was carried out with diluted full-length PCR products by Accuprime Taq DNA polymerase High Fidelity (Invitrogen). Quantitative PCR was carried out as previously described.[3] The specific primer sets for each PCR are described in Table S2.

Immunoblot analysis. Cells were collected, washed with PBS, and lysed with RIPA buffer. For immunoprecipitation, cells were lysed with TNE buffer and incubated with specific antibody. Proteins samples were then analyzed by immunoblots with specific antibodies: anti-tubulin, anti-Ikaros, and anti-Helios antibodies were from Santa Cruz Biotechnology (Santa Cruz, CA, USA). Mouse anti-FLAG antibody (M2) was from Sigma-Aldrich (St. Louis, MO, USA). Rabbit polyclonal anti-HA

[7]To whom correspondence should be addressed.
E-mail: tnabe@ims.u-tokyo.ac.jp

doi: 10.1111/cas.12181
© 2013 Japanese Cancer Association

antibody was from MBL (Nagoya, Japan). Anti-mouse, rabbit, and goat secondary antibodies were from Promega (Fitchburg, WI, USA).

Immunostaining. HeLa cells were cultured on coverslip slides and transfected with the indicated expression vectors by Lipofectamine LTX (Invitrogen). At 24 h post transfection, cells were washed three times with PBS, fixed in 4% paraformaldehyde, and permeabilized with 0.1% Triton X-100. Then, cells were stained with primary antibodies (diluted 1:500 to 1:2000). Alexa-488 or 546-conjugated secondary antibodies (Molecular Probes, Life Technologies, Carlsbad, CA, USA) were used for detection of specific targets, and DAPI was used for nuclear staining. Images were acquired by using a Nikon A1 confocal microscope (Nikon, Tokyo, Japan).

Electrophoretic mobility-shift assay. Experimental conditions and detail methods were previously reported.[3] For evaluation of DNA binding activity, 3–5 μg nuclear extracts from each transfectant were used per each lane of electrophoresis. The oligonucleotide sequences used as a probe are provided in Table S2.

Luciferase assay. The pGL4.10-firefly vector (Promega) containing *Hes1* promoter was used as a reporter vector and RSV-renilla vector was used as a control vector. HeLa cells were transiently transfected with these reporters and each Ikaros or/and Helios expression vector by Lipofectamine 2000 reagent (Invitrogen). The luciferase activities were quantified by the Dual-Luciferase Reporter Assay System (Promega) at 24 h post-transfection.

Retroviral construction and transduction. The FLAG-Hel-5 cDNA sequence was subcloned into retrovirus vector pRx-puro. Stable cell populations expressing Hel-5 were selected by puromycin. The shRNA-expressing retroviral vectors and virus production procedures have been established.[3] The shRNA sequences are listed in Table S2. Stable cell populations were obtained by puromycin or G418 selection.

Proliferation assays. Cells (0.5 or 1.0×10^4) were plated in 96-well plates with media supplemented with 10% or 0.2% FCS. The cell numbers were evaluated for 4 days by Cell Counting Kit-8 (Dojindo, Kumamoto, Japan). The averages of at least three independent experiments are shown.

Gene expression microarray analyses. Gene expression microarray used the 4×44K Whole Human Genome Oligo Microarray (Agilent Technologies, Santa Clara, CA, USA); detailed methods were previously reported.[3] Coordinates have been deposited in the Gene Expression Omnibus database with accession numbers GSE33615 (gene expression microarray), GSE33602 (copy number analyses), and GSE41796 (Jurkat models).

Results

Abnormal expression of short Helios transcripts in primary ATL cells. To characterize the gene expression signature in primary ATL cells, we previously carried out mRNA microarray analyses on a large number of samples. The comprehensive survey unveiled deregulated expression of Ikaros family genes; transcription levels of Ikaros and Aiolos were downregulated in ATL samples, whereas Helios was upregulated (Fig. S1). Thus, we examined the detailed expression patterns and levels of Ikaros family members in PBMCs derived from a panel of ATL patients and HTLV-1 carriers (Fig. 1a). Compared with control PBMCs from normal volunteers (Fig. 1b), the expression levels of Ikaros and Aiolos seemed to be downregulated in ATL samples, consistent with our microarray results. However, there were obvious abnormalities in the expression patterns of Helios. The main isoform of Helios was changed from full-length Hel-1 to Hel-2, which lacks exon 3 that contains the first N-terminal zinc finger in the DNA-binding domain. In addition, four ATL-specific Helios short transcripts were identified (Fig. 1c). Among them, Hel-5 and Hel-6 have been reported to be expressed in ATL.[29] We also identified two novel variants, Hel-v1 that lacks exons 3 and 4 and Hel-v2 that lacks exons 2, 3, and 6. These abnormal Helios variants were also expressed in the samples of high-risk HTLV-1 carriers, who subsequently developed ATL in the next few years. Furthermore, nested PCR revealed that Hel-5 or Hel-6 were expressed in a majority of ATL samples (17/22 acute cases, 10/10 chronic cases, and 5/5 smoldering cases; total, 32/37 cases) (Fig. 1d, upper panels), whereas Hel-v1 was expressed only in limited cases of ATL (Fig. 1d, lower panels). In four cases, Helios was not expressed. Collectively, our mRNA analysis showed that Helios expression was generally deregulated in ATL cells.

Genomic abnormalities at the *Helios* locus in primary ATL cells. To investigate the *Helios* locus in ATL, we retrieved data from our gene copy number analysis[3] and found that specific genomic deletion was accumulated at the *Helios* locus in ATL samples (17/168 cases, Fig. 2). All 17 cases were aggressive-type ATL (12/17 lymphoma types and 5/17 acute types). Furthermore, we found that two acute ATL cases in Figure 1(a) (#9 and #14), which showed severely deregulated or lost Helios expression, had a genomic deletion of the *Helios* locus.

Dimerization ability of ATL-type Helios isoforms with wild-type Helios or Ikaros. Consistent with a previously published report,[33] co-immunoprecipitation analyses confirmed that wild-type Hel-1 formed homodimers with themselves and heterodimers with wild-type Ikaros (Ik-1) protein (Fig. 3a, top panel, lane 1 and lane 4). In contrast, the dimerization activity of another artificial Helios mutant (Hel-ΔC), which lacks the dimerization domain at the C-terminal region, was dramatically declined (Fig. 3b, top panel, lane 1 and lane 4). We confirmed that all ATL-type Helios proteins could interact with Hel-1 and Ik-1, despite the fact that all of them lack various sets of the N-terminal exons (Fig. 3c–f).

Cytoplasmic localization of ATL-type Helios isoforms lacking exon 6. Ectopically expressed Hel-1 and Ik-1 were localized in the nucleus (Fig. 4a, top two panels). Regarding the ATL-type Helios isoforms, we found that Hel-5 and Hel-v1 were localized in the nucleus, whereas Hel-6 and Hel-v2, both of which lack exon 6, were substantially localized in the cytoplasm (Fig. 4a, middle four panels). We also confirmed the cytoplasmic localization of Hel-Δexon 6, which is an artificial Helios mutant lacking only exon 6 (Fig. 4a, bottom panel). Thus, exon 6 appears to be critical for nuclear localization of Helios proteins. Furthermore, defect of exon 6 led to disruption of the

Fig. 1. (On the next page) Abnormal expression of Helios mRNA in primary adult T-cell leukemia (ATL) cells. (a) Expression analysis of Ikaros family genes in PBMCs by full-length RT-PCR (Acute, $n = 22$; Chronic, $n = 10$; Smoldering, $n = 5$; HTLV-1 carriers, $n = 5$; High-risk carriers, $n = 4$). To detect and distinguish alternative splicing variants, PCR analyses were carried out with the sense and antisense primer sets designed in the first and final exons of each full-length transcript of Ikaros family genes. Obtained cDNAs were cloned and their sequences were analyzed. The samples acute #4, 4′, and 4″ were derived from the same patient, but were studied independently. (b) Expression of Ikaros family genes in PBMCs from normal volunteers ($n = 10$). (c) Schematic representation of Hel-1, Hel-2, and ATL-type Helios isoforms identified in this study. Hel-variant 1 (Hel-v1) and Hel-variant 2 (Hel-v2) are novel isoforms in ATL. Arrows indicate primer locations of full-length PCR for Helios. Ex, exon; F1–F6, functional zinc-finger domains. (d) Nested PCR with specific primer sets, which were designed at exon junction of exon 1–5 or exon 2–5 for detection of Hel-5 and Hel-6 (upper panel), or detection of Hel-v1 (lower panel), respectively. Arrows indicate primer locations.

doi: 10.1111/cas.12181
© 2013 Japanese Cancer Association

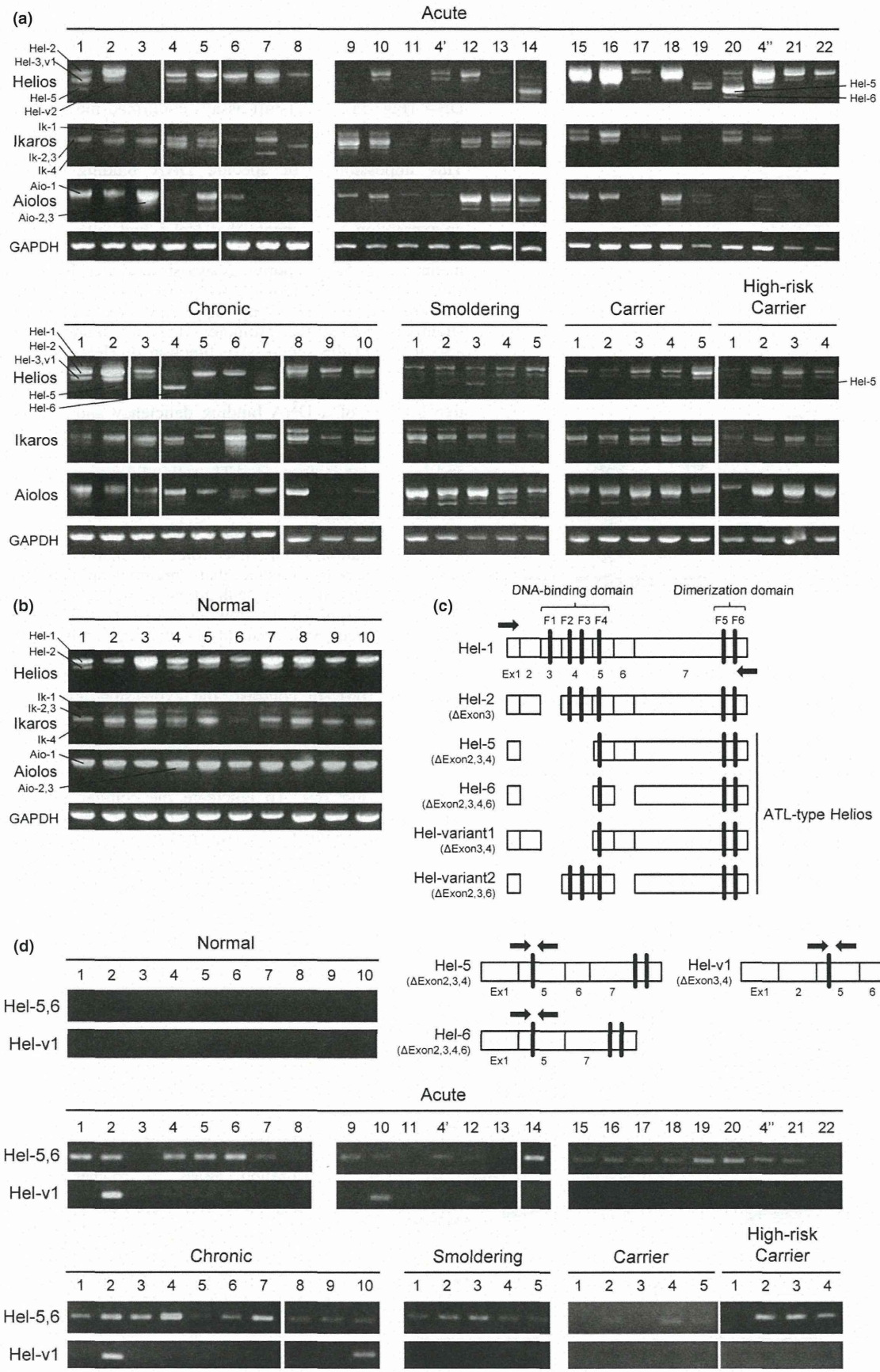

© 2013 Japanese Cancer Association

cellular localization of binding partners. When Hel-6 or Hel-v2 were co-expressed with Hel-1 or Ik-1, they were co-localized in the cytoplasm (Fig. 4b, Fig. S2).

Dominant-negative function of ATL-type Helios isoforms against wild-type Helios and Ikaros. We next examined the functional aspects of these ATL-type Helios isoforms by evaluating their DNA-binding capacities. For EMSA, we used an oligonucleotide probe derived from the promoter region of human *Hes1*, which was a direct target of Ikaros.[34,35] Ectopically expressed Hel-1 or Ik-1 could bind human *Hes1* promoter DNA (Fig. 5a). Supershift assays confirmed the binding specificity (Fig. 5b). In contrast, all ATL-type Helios isoforms did not show any specific binding to the *Hes1* promoter (Fig. 5a). This impossibility of specific DNA binding of ATL-type Helios was confirmed with another independent DNA probe, IkBS4[33,36] (data not shown). In addition, it was found in co-expression experiments that Hel-5 had antagonistic effects on the DNA binding capacity of Ik-1 in a dose-dependent manner (Fig. 5c). Reporter assays showed that Hel-1 and Ik-1 suppressed *Hes1* promoter activity. However, ATL-type Helios isoforms did not show any suppressive activity, and actually slightly activated the promoter (Fig. 5d). Furthermore, they also inhibited the suppressive function of Hel-1 and Ik-1 in a dose-dependent manner (Fig. 5e, Fig. S3). These data clearly indicate that ATL-type Helios isoforms are functionally defective because of a DNA binding deficiency and act dominant-negatively in transcriptional suppression induced by Hel-1 or Ik-1. We also confirmed that Hel-2, which lacks only exon 3 and is a major isoform in ATL cells, did not possess suppressive activity against *Hes1* promoter in spite of having binding activity (Fig. 5a,d).

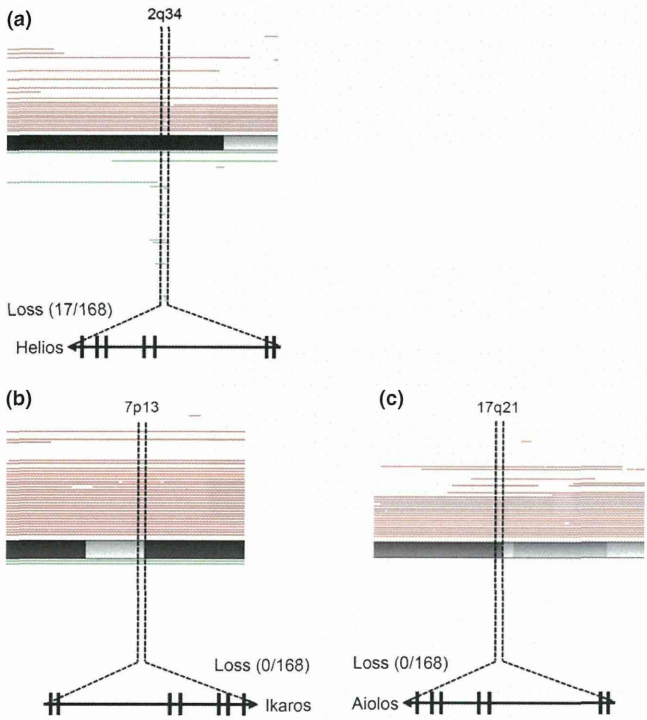

Fig. 2. Genetic abnormalities in *Helios* locus in primary adult T-cell leukemia cells. The results of our copy number analyses[3] (total number, $n = 168$; acute type, $n = 35$; chronic type, $n = 41$; lymphoma type, $n = 44$; smoldering type, $n = 10$; intermediate, $n = 1$; unknown diagnosis, $n = 37$). Tumor-associated deletion of *Helios* region (17/168) was detected (a). No specific genomic losses were observed in *Ikaros* (b) or *Aiolos* loci (c). Recurrent genetic changes are depicted by horizontal lines based on Copy Number Analyser for GeneChip output of the single nucleotide polymorphism array analysis.

Major ATL-type Helios variant, Hel-5, promotes T cell growth. Given the tumor-suppressive roles of Ikaros family members,[12–15] it was expected that abnormal splicing of Helios could contribute to T cell leukemogenesis. The mRNA level of Helios was significantly downregulated in ATL-related cell lines compared with that in T-cell lines without HTLV-1 (Fig. 6a, Fig. S4). Moreover, Helios protein was not detected in any ATL-derived or HTLV-1-infected cell lines used in this study (Fig. 6b). In contrast, the expression levels of Ikaros mRNA did not show major differences between HTLV-1-infected and uninfected T-cell lines. Those of Aiolos were low in most cell lines irrespective of HTLV-1 infection (Fig. 6a, Fig. S4). Ikaros protein was detected in all T-cell lines used in this study (Fig. 6b). To elucidate the cellular effects of the expression of dominant-negative ATL-type Helios isoforms in T cells, we established stable Jurkat cells expressing Hel-5 (Fig. 6c). A cell proliferation assay confirmed that Hel-5 expression significantly promoted Jurkat cell proliferation

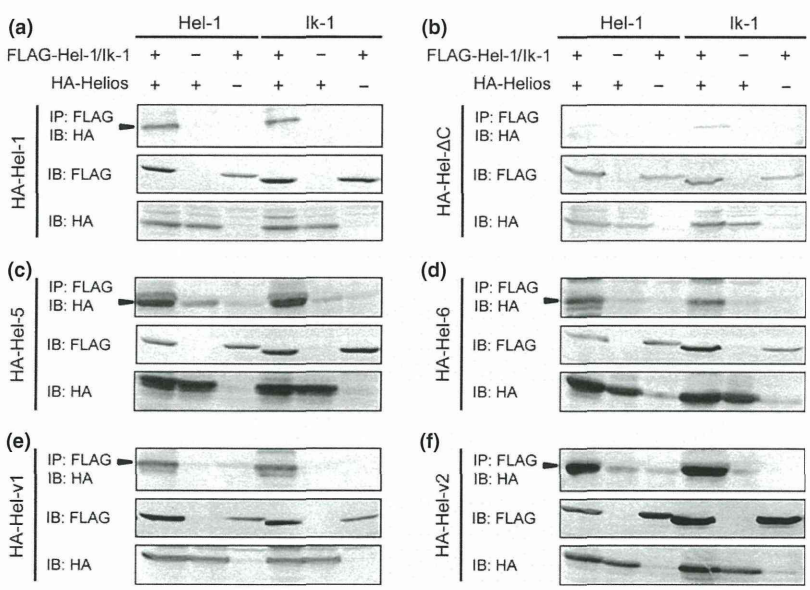

Fig. 3. Dimerization ability of adult T-cell leukemia (ATL)-type Helios isoforms. *In vitro* dimerization assays by co-immunoprecipitation between ATL-type Helios and wild-type Helios or Ikaros proteins. 293T cells were transfected with the indicated combination of expression vectors and subjected to co-immunoprecipitation analyses (top panels). Arrowheads indicate the complex of FLAG and HA-tagged proteins. Middle and bottom panels show the input samples. Hel-1 (a) and Hel-ΔC (b) included as positive and negative controls, respectively. ATL-specific isoforms, Hel-5 (c), Hel-6 (d), Hel-v1 (e), and Hel-v2 (f) were tested. IB, immunoblot; IP, immunoprecipitant.

doi: 10.1111/cas.12181
© 2013 Japanese Cancer Association